Dark Matter Models Beyond the WIMP Paradigm

Michael J. Baker
Johannes Gutenberg University, Mainz, Germany

Summary. — Thermal freeze-out of a weakly interacting massive particle is the dominant paradigm for dark matter production. This scenario is now being probed by direct and indirect detection experiments, as well as at colliders. The lack of convincing signals motivates us to consider alternative scenarios. In this contribution we discuss a scenario where the dark matter abundance is controlled by a 'vev flip-flop', which sets the relic abundance via a period of dark matter decay just before electroweak symmetry breaking. We describe the mechanism and show that it is successful in a wide range of parameter space before discussing detection possibilities.

PACS 95.35.+d – Dark matter.
PACS 12.60.Fr – Extensions of Higgs sector.

1. – Introduction

Uncovering the nature of Dark Matter (DM) is one of the clearest open problems in modern physics. Its existence has been well established by a wide range of observations and many of its properties are now well characterised. These include both measurements of its local density, from the motions of gas, stars and galaxies, and its average density, primarily from observations of the cosmic microwave background. However, these measurements have only observed DM through its gravitational interaction.

The leading candidate for DM is a Weakly Interacting Massive Particle (WIMP). This picture assumes a new, heavy particle which is in thermal and chemical equilibrium in the early universe. As the temperature drops below the mass of the particle, interactions annihilating the particle occur more often than those producing the particle and its abundance drops. As the abundance drops, the annihilation rate also reduces. This continues until the annihilation rate becomes smaller than the expansion rate of the universe, at which point the particles can no longer annihilate and they 'freeze-out'. The WIMP miracle is the observation that, with weak scale masses and order one couplings, the subsequent relic abundance is approximately the same as the observed relic abundance of DM. Further to this, supersymmetry as a solution to the hierarchy problem suggests several new particles around the weak scale which could possibly account for

DM. These coincidences led to the supersymmetric neutralino becoming the archetypal DM candidate.

This picture has motivated and shaped a wide ranging experimental effort to search for WIMPs via their non-negligible couplings to Standard Model (SM) particles. These efforts are based on DM annihilation in galaxies and galaxy clusters (indirect detection), scattering of DM particles on atomic nuclei (direct detection), and production of WIMPs or associated particles at colliders. The sensitivity of these experiments has increased dramatically in recent years, predominantly with larger scale direct detection experiments and with the advent of the LHC, and large regions of the neutralino parameter space are being probed. The lack of any convincing signal [1–7] has motivated theorists to develop alternative mechanisms to explain the observed DM abundance.

Alternatives to WIMP dark matter should provide a DM candidate which interacts very weakly with electromagnetic radiation, which is cosmologically stable, and which has the observed relic abundance. Structure formation simulations also suggest that DM should have been non-relativistic at the beginning of galaxy formation. Widely discussed candidates are:

- **WIMPless Dark Matter** - A variation on WIMP thermal freeze-out, where the connection to the weak scale is dropped. A common origin of mass and coupling to the thermal bath can mean that thermal freeze-out still produces the observed relic abundance [8].

- **Axions** - Originally a solution to the strong CP problem [9], they could account for DM with their relic abundance being set by an initial misalignment angle and their decay constant, see [10] for a recent review.

- **Sterile Neutrinos** - These inert fermions can be produced by resonant and non-resonant mixing with active neutrinos or by the decay of heavier particles, resulting in either cold or warm dark matter candidates. For a recent review, see [11].

- **Freeze-in** - In this scenario, a decoupled particle with negligible abundance in the very early universe may be produced via very weak interactions with the thermal bath until the temperature of the Universe drops below the mass of the particle [12, 13].

- **SIMPs and ELDERs** - A variety of models, e.g, [14–16], assume a strongly self-interacting dark matter candidate which can undergo $n \to 2$ processes ($n \geq 3$) purely within the dark sector. For SIMPs the dark sector must couple weakly to the SM sector to maintain thermal equilibrium, while for ELDERs the DM thermally decouples from the SM bath before their own self-interactions freeze-out.

- **Primordial Black Holes** - To account for DM these must have formed before Big-Bang nucleosynthesis. Recent measurements of $\sim 30 M_\odot$ black holes at LIGO have fuelled recent interest that these may account for DM, e.g. [17].

In this contribution, we discuss a new scenario in which the DM abundance is set not by annihilation, but by decay. We imagine that there is a dark matter candidate which couples very weakly to the thermal bath, which freezes-out when relativistic and is subsequently overproduced in the early universe. We imagine that this particle is charged under a symmetry so that it cannot decay while the symmetry remains intact. We further imagine that there is a new scalar which is charged under the symmetry

Field	Spin	SM	$\mathbb{Z}_3$	mass scale
χ	$\frac{1}{2}$	$(1,1,0)$	$\chi \to e^{2\pi i/3}\chi$	TeV
S_3	0	$(1,3,0)$	$S_3 \to e^{2\pi i/3}S_3$	100 GeV
Ψ_3	$\frac{1}{2}$	$(1,3,0)$	$\Psi_3 \to e^{-2\pi i/3}\Psi_3$	TeV
Ψ_3'	$\frac{1}{2}$	$(1,3,0)$	$\Psi_3' \to e^{-2\pi i/3}\Psi_3'$	TeV

TABLE I. – *The new particle content of our toy model along with their spin, their charges under the SM gauge group $SU(3)_c \times SU(2)_L \times U(1)_Y$ and the dark sector global symmetry $\mathbb{Z}_3$, and their mass scales.*

which stabilises the DM. This scalar can couple to the SM Higgs and the resulting scalar potential may undergo multiple phase transitions, 'flip-flopping' between phases in which the symmetry stabilising the DM is unbroken and a phase where it is broken. During the broken phase, the initially overabundant DM particles decay and are depleted, resulting in the relic abundance observed today.

This picture of an initial overabundance followed by a period of DM decay around the weak scale is quite general and one can imagine many realisations of this mechanism. Indeed, the 'vev flip-flop' could impact DM in various ways beyond the decay mechanism discussed here.

2. – Model Framework

The new particle content of our toy model is shown in table I. We take our DM candidate χ to be a Dirac fermion which is a gauge singlet under the SM gauge group. It is charged under a $\mathbb{Z}_3$ symmetry, which acts to stabilise the DM. There is a complex scalar S_3 which is a triplet under the SM $SU(2)_L$ gauge group. When this scalar obtains a vev, it breaks the stabilising $\mathbb{Z}_3$ symmetry. Two new fermions, Ψ_3 and Ψ_3', are introduced which are also triplets under the SM $SU(2)_L$ gauge group. When S_3 obtains a vev, χ will be able to decay by mixing into Ψ_3 and Ψ_3' and decaying via the weak force.

The new Yukawa terms in the Lagrangian of this model are

$$\mathcal{L}_{\rm Yuk} = y_\chi S_3^\dagger \bar{\chi}\Psi_3 + y_\chi' S_3^\dagger \bar{\chi}\Psi_3' + y_\Psi \epsilon^{ijk} S_3^i \overline{\Psi_3^j}(\Psi_3'^k)^c + h.c. \tag{1}$$

The first two terms are the only terms which connect χ to particles in the thermal bath. It is technically natural for these couplings to be arbitrarily small, and we will assume $y_\chi \sim y_\chi' \lesssim 10^{-7}$. This is small enough to ensure that χ decouples while it is relativistic. So that χ doesn't decay within the dark sector we also assume that $m_\chi < m_S + m_\Psi$ at $T = 0$ for all possible components of S_3 and $\Psi_3^{(\prime)}$. We assume $y_\Psi \sim 1$ so that Ψ_3 and Ψ_3' are efficiently depleted by usual thermal freeze-out mechanism.

The tree level scalar potential is

$$\begin{aligned} V^{\rm tree} = & -\mu_H^2 H^\dagger H + \lambda_H (H^\dagger H)^2 - \mu_S^2 S_3^\dagger S_3 + \lambda_S (S_3^\dagger S_3)^2 + \lambda_3 (S_3^\dagger T^a S_3)^\dagger (S_3^\dagger T^a S_3) \\ & + \alpha (H^\dagger H)(S_3^\dagger S_3) + \beta (H^\dagger \tau^a H)(S_3^\dagger T^a S_3)\,, \end{aligned} \tag{2}$$

The first line in eq. (2) contains the usual SM Higgs potential, where we write $H = (G^+, (h + iG^0)/\sqrt{2})$, and the analogous potential for the scalar mediator $S_3 = (s^+, (s + ia)/\sqrt{2}, s^-)$, where an extra quartic coupling is possible as S_3 is a triplet. The second

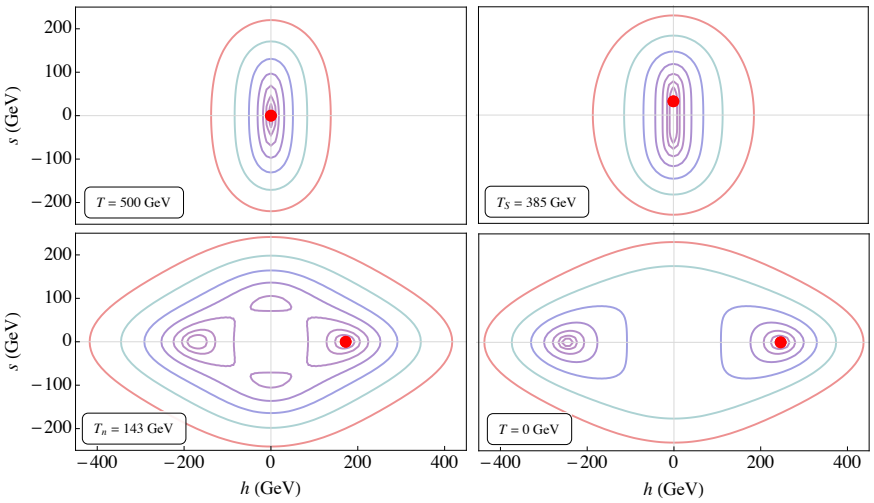

Figure 1. – The effective potential at high T where the Universe is in the symmetric phase (top left), at the temperature of the first phase transition where S_3 obtains a vev (top right), at the second phase transition where the S_3 vev goes to zero and the SM Higgs obtains a vev (bottom left), and at the present time (bottom right). The red dots indicate the phase of the Universe at each stage. The contours are evenly spaced on a log scale and range from $1.4 \times 10^6\,\mathrm{GeV}^4$ (purple) to $5.6 \times 10^8\,\mathrm{GeV}^4$ (red). In this plot, $\lambda_S = \lambda_3 = 1$, $\alpha = 1.33$, $\beta = 0$, and $m_s = 185\,\mathrm{GeV}$ at $T = 0\,\mathrm{GeV}$.

line contains two Higgs portal terms with couplings α and β. We make the assumption that $\beta \sim 0$, otherwise a tree level mass splitting shifts the mass of s^+ (s^-) downward (upward) and gives a stable, charged relic (which is very strongly constrained). This assumption is stable under radiative corrections [18].

3. – The Vev Flip-Flop

To study the behaviour in the early universe we calculate the effective potential in finite temperature QFT. We choose the convention that only the electrically neutral, CP even components h and s of H and S_3 acquire vevs. We can then write the effective potential as a function of these components and tree level Lagrangian couplings. In addition to V^{tree}, the effective potential includes the T-independent one-loop Coleman–Weinberg contributions [19], the one-loop T-dependent corrections [20], and the resummed higher-order 'daisy' contributions [21–24], see [25] for details.

In fig. 1 we show the effective potential for a particular choice of Lagrangian parameters, see caption. At high T (top left), V^{eff} is symmetric in both h and s and the universe is in a phase where neither h nor s have a vev. As the Universe cools the T-dependent contributions become less important and, since μ_S^2 is positive, S_3 develops a vev at $T = T_S$ (top right). As the $\mathbb{Z}_3$ symmetry is now broken, χ can decay. The mass of S_3 depends directly on temperature, while the masses of $W^\pm$ and the charged components of $\Psi_3^{(\prime)}$ depend on the vev of S_3, so various decay modes can also be opened and closed kinematically.

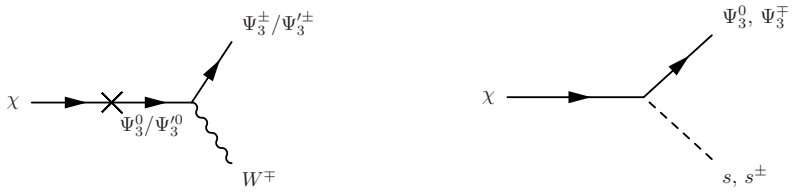

Figure 2. – Feynman diagrams showing possible decay modes of χ. Decay modes involve mixing with $\Psi_3^{(\prime)}$ (left) or may be kinetically allowed at $T \neq 0$ (right).

As the temperature continues to drop V^{eff} develops new minima at non-zero $\langle h \rangle$. At these minima the extra contribution changes the sign of the S_3 mass parameter, $-\mu_S^2 S_3^\dagger S_3 + \alpha(H^\dagger H)(S_3^\dagger S_3) \to (-\mu_S^2 + \alpha\langle h \rangle^2) S_3^\dagger S_3$, so $\langle s \rangle = 0$ is restored at the new minima. This phase transition is first order as there is a barrier between the $\langle h \rangle \neq 0$ and the $\langle s \rangle \neq 0$ minima. This transition takes place when the growth of bubbles of the new phase is energetically favourable [26], which happens at $T = T_n$. To calculate the phase transition temperatures T_S and T_n we used the publicly available `CosmoTransitions` package [27–30]. The effective potential at T_n is shown in the bottom left panel of fig. 1. At this point $\langle s \rangle = 0$ so the $\mathbb{Z}_3$ symmetry is restored and the dark sector stabilises. After this, the $\langle h \rangle \neq 0$ minima deepen and the Universe remains in the $\langle h \rangle \neq 0$ phase, (bottom right).

4. – Dark Matter Abundance

We imagine that a thermal abundance of DM is produced by some new physics at a scale far above the electroweak scale. Since χ couples very weakly to the thermal bath, it freezes-out when it is still relativistic and its abundance is around 10 orders of magnitude too large to account for the observed abundance of DM.

When S_3 obtains a vev, the first two Yukawa terms in eq. (1) lead to a mixing between χ and $\Psi_3^{(\prime)}$. This provides a decay mode for χ, via $\chi \to W\Psi_3$ and $\chi \to W\Psi_3'$, shown in fig. 2 (left). The masses of the scalar particles depend on thermal effects, while the S_3 vev shifts the masses of the charged components of $\Psi_3^{(\prime)}$. This means that although the decay of χ to the charged components of S_3 and $\Psi_3^{(\prime)}$ is kinematically forbidden at $T = 0$, it may be possible at finite T. This process is shown in fig. 2 (right).

To track the abundance of χ during the vev flip-flop, we solve the Boltzmann equation

$$\dot{n}_\chi + 3Hn_\chi = -\frac{\Gamma}{\gamma}\left(n_\chi - n_\chi^{\text{eq}}\right) \tag{3}$$

together with the Friedmann equation

$$H^2 = \left(\frac{\dot{a}}{a}\right)^2 = \frac{8\pi G_N}{3}\left(\rho_{\text{SM}} + \rho_\chi\right). \tag{4}$$

This is similar to the Boltzmann equation relevant for thermal freeze-out, except the number densities appear to the first and not the second power, and the thermally averaged cross section is replaced by the decay rate divided by the relativistic gamma factor. The

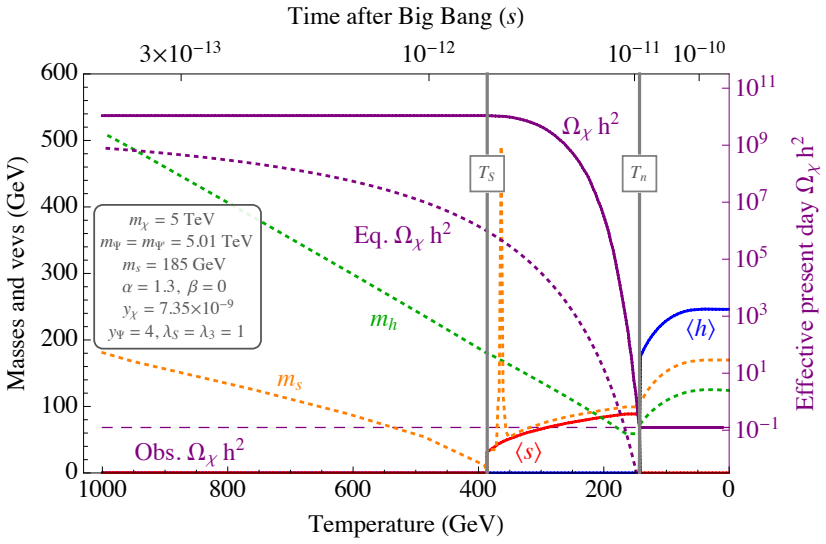

Figure 3. – The vev flip-flop: around $T = 1\,\text{TeV}$, both the the S_3 vev $\langle s \rangle$ (solid red) and the SM Higgs field vev $\langle h \rangle$ (solid blue) are zero. There is a phase transition at $T_S = 385\,\text{GeV}$ where S_3 develops a nonzero vev. At this point the $\mathbb{Z}_3$ symmetry breaks and the dark sector destabilises. The evolution of the effective present day relic density is shown in solid purple, obtained from scaling the instantaneous DM number density by the subsequent expansion of the Universe. There is a second phase transition at $T_n = 143\,\text{GeV}$ where h develops a vev and $\langle s \rangle$ goes to zero, restoring the $\mathbb{Z}_3$ symmetry and stabilising the DM. The observed relic abundance (dashed purple) and DM equilibrium density (dotted purple), along with the SM Higgs mass m_h (dotted green) and s mass m_s (dotted orange), are also given.

decay rate Γ depends on temperature through m_s, m_h and $\langle s \rangle$, while the relativistic gamma factor depends on momentum. The time dilation of high momentum particles turns out to be an important effect and we take account of this by discretising into momentum bins, see [25] for details.

We show the evolution of the vevs, the scalar masses and the effective present day DM relic density as the Universe cools in fig. 3, for an illustrative benchmark point. The parameters of the scalar potential are the same as in fig. 1. At $T = 1\,\text{TeV}$, the χ relic density is constant, as χ cannot decay, and is around ten orders of magnitude too large. This continues until the phase transition at $T_S \sim 385\,\text{GeV}$ where s obtains a non-zero vev and χ begins to decay. Since $T \sim t^{-1/2}$ in a radiation dominated universe, most χ decays happen at low temperatures, just above the second phase transition. At $T_n \sim 143\,\text{GeV}$ the Universe nucleates to the $\langle s \rangle = 0$, $\langle h \rangle \neq 0$ phase with a first order phase transition. At this point the $\mathbb{Z}_3$ symmetry is restored and $m_\chi < m_S + m_\Psi$ so DM decays are no longer possible.

5. – Parameter Space

In fig. 4 we show the m_s–α slice of parameter space. The solid red and black lines show tree level estimates of where the vev flip-flop should occur. Below the black line, μ_S^2 is negative at tree level, so S_3 doesn't obtain a vev. Above the red line, $\mu_S^2 > 0$

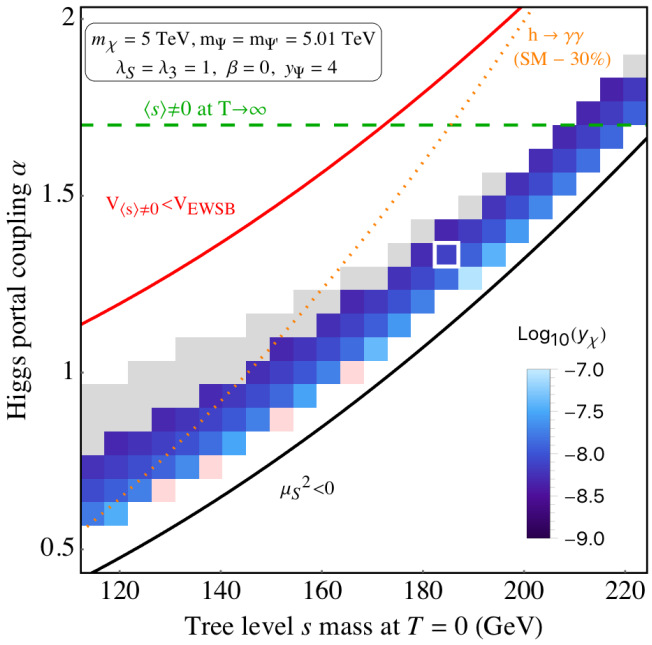

Figure 4. – The value of $y_\chi = y'_\chi$ which yields the observed DM relic density. The vev flip-flop occurs for all the pixelated points, including those plotted in grey and pink (which do not yield the correct relic density). Tree level estimates for where the flip-flop occurs are given by the solid red and black lines. Above the dotted orange line, the decay rate for $h \to \gamma\gamma$ is more than 30% lower than the SM prediction. The $\mathbb{Z}_3$ symmetry is broken in the high T limit above the dashed green line.

is so large that the Universe never leaves the $\langle s\rangle \neq 0$, $\langle h\rangle = 0$ phase. The pixellated region shows where the vev flip-flop occurs for the one-loop effective potential detailed in [25]. The blue colour-coded region shows points for which we can obtain the correct relic abundance, with the corresponding shade indicating the required value of $y_\chi = y'_\chi$. We see that this is usually possible if the vev flip-flop happens at all. Although we cannot obtain the correct relic abundance for the points shown in grey and pink, these points can be recovered by shifting m_χ or other parameters. Above the dashed green line, our model is in the phase with $\langle s\rangle \neq 0$ in the $T \to \infty$ limit. In principle, χ decays are then sensitive to higher scale physics, but our calculations remain valid since most decays happen just above the electroweak phase transition.

6. – Constraints and Future Tests

We now turn to possible tests of the scenario outlined above. Since the dominant DM component χ couples only very weakly to dark sector particles, and to SM particles only via loops of these particles, the direct and indirect signals of χ will be very small.

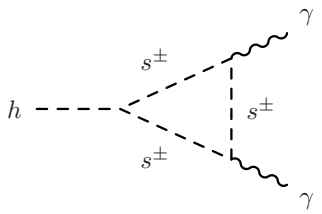

Figure 5. – Feynman diagram showing the contribution of the charged components of S_3 to $h \to \gamma\gamma$.

A better prospect is detecting signals from the subdominant populations of S_3, Ψ_3 and Ψ_3', which will none-the-less remain challenging.

At the LHC or a possible future collider, $s^\pm$ pairs may be produced via Drell–Yan production, which will go on to decay via $s^\pm \to s + W^{*\pm}$. The mass splitting between the charged and neutral components of S_3 is ~ 160 MeV, so the decay products will typically be too soft to detect. Since this mass splitting is above the pion threshold, the typical decay length remains small and disappearing charged tracks searches may be possible but challenging. Simple mono-X searches are currently several orders of magnitude too weak to probe the parameter space.

Perhaps the most promising probe is the precision measurement of the $h \to \gamma\gamma$ rate. As shown in fig. 5, the charged components of S_3 contribute to this decay and in fact destructively interfere with the SM contribution, resulting in a reduced $h \to \gamma\gamma$ rate. In fig. 4 we show the region where the deviation from the SM rate is greater than 30 %, which corresponds to approximately 2 σ at the current sensitivity [31–34]

7. – Summary

In this contribution we have highlighted a range of alternatives to the thermal WIMP paradigm, before discussing a new mechanism which accounts for the observed dark matter abundance via a period of decay just before electroweak symmetry breaking. The addition of a new scalar can lead to a 'vev flip-flop', where this new scalar obtains a vev for some time before returning to its symmetric phase when the SM Higgs obtains a vev. If this scalar is charged under the symmetry which stabilises the dark sector, its vev can lead to DM decay. We have shown that this mechanism can successfully account for the observed DM relic abundance in wide range of parameter space. We have discussed possible tests of this model, focussing on the best prospects at colliders.

8. – Acknowledgements

It is a great pleasure to thank the organisers of Les Rencontres de Physique de la Vallée d'Aoste for a stimulating workshop with engaging talks and interesting discussions. The work presented here was completed as part of a fruitful and enjoyable collaboration with Joachim Kopp. This proceeding was written with kind hospitality provided by Fermilab and support from an invisiblesPlus secondment. This work was in part supported by the German Research Foundation (DFG) under Grant Nos. KO 4820/1–1 and FOR 2239, and by the European Research Council (ERC) under the European Union's Horizon 2020 research and innovation programme (grant agreement No. 637506, "νDirections").

References

[1] LUX Collaboration, *Phys. Rev. Lett.*, **118** (2017) 2.
[2] PandaX-II Collaboration, *Phys. Rev. Lett.*, **117** (2016) 12.
[3] Fermi-LAT Collaboration, *Phys. Rev. Lett.*, **115** (2015) 23.
[4] AMS-02, *EPJ Web Conf.*, **121** (2016) 03006.
[5] Madhavacheril M.S., Sehgal N. and Slatyer T.R., *Phys. Rev.*, **D89** (2014) 103508.
[6] ATLAS Collaboration, *Phys. Rev.*, **D94** (2016) 3.
[7] CMS Collaboration, *CMS-PAS-EXO-16-037* (2016).
[8] Feng J.L. and Kumar J., *Phys. Rev. Lett.*, **101** (2008) 231301.
[9] Peccei R.D. and Quinn H.R., *Phys. Rev. Lett.*, **38** (1977) 1440-1443.
[10] Duffy L.D. and van Bibber K., *New J. Phys.*, **11** (2009) 105008.
[11] Drewes, M. et al., *JCAP*, **1701** (2017) 01.
[12] McDonald J., *Phys. Rev. Lett.*, **88** (2002) 091304.
[13] Hall L.J. et al., *JHEP*, **03** (2010) 080.
[14] Hochberg Y. et al., *Phys. Rev. Lett.*, **113** (2014) 171301.
[15] Hochberg Y. et al., *Phys. Rev. Lett.*, **115** (2015) 2.
[16] Kuflik E. et al., *Phys. Rev. Lett.*, **116** (2016) 22.
[17] Bird S. et al., *Phys. Rev. Lett.*, **116** (2016) 20.
[18] Kopp J. et al., *Phys. Dark Univ.*, **2** (2013) 22-34.
[19] Coleman S.R. and Weinberg E.J., *Phys. Rev.*, **D7** (1973) 1888-1910.
[20] Dolan L. and Jackiw R., *Phys. Rev.*, **D9** (1974) 3320-3341.
[21] Carrington M.E., *Phys. Rev.*, **D45** (1992) 2933-2944.
[22] Quiros M., *Proceedings, Summer School in High-energy physics and cosmology: Trieste, Italy, June 29-July 17, 1998*, (1999) 187-259.
[23] Ahriche A., *Phys. Rev.*, **D75** (2007) 083522.
[24] Delaunay C., Grojean C. and Wells J.D., *JHEP*, **04** (2008) 029.
[25] Baker M.J. and Kopp J., arXiv:1608.07578 (2016).
[26] Linde A.D., *Nucl. Phys.*, **B216** (1983) 421.
[27] Wainwright C.L., *Comput. Phys. Commun.*, **183** (2012) 2006-2013.
[28] Kozaczuk J. et al., *JHEP*, **01** (2015) 144.
[29] Blinov N. et al., *Phys. Rev.*, **D92** (2015) 3.
[30] Kozaczuk J., *JHEP*, **10** (2015) 135.
[31] ATLAS and CMS Collaborations, *JHEP*, **08** (2016) 045.
[32] Particle Data Group, *Chin. Phys.*, **C40** (2016) 10.
[33] CMS Collaboration, *CMS-PAS-HIG-16-020* (2016).
[34] ATLAS Collaboration, *ATLAS-CONF-2016-067* (2016).